Developmental Cell
Article

The Disulfide Relay of the Intermembrane Space Oxidizes the Ribosomal Subunit Mrp10 on Its Transit into the Mitochondrial Matrix

Sebastian Longen,[1] Michael W. Woellhaf,[1] Carmelina Petrungaro,[2] Jan Riemer,[2] and Johannes M. Herrmann[1,*]
[1]Division of Cell Biology, Department of Biology, University of Kaiserslautern, Erwin-Schrödinger-Strasse 13, 67663 Kaiserslautern, Germany
[2]Division of Cellular Biochemistry, Department of Biology, University of Kaiserslautern, Erwin-Schrödinger-Strasse 13, 67663 Kaiserslautern, Germany
*Correspondence: hannes.herrmann@biologie.uni-kl.de
http://dx.doi.org/10.1016/j.devcel.2013.11.007

SUMMARY

Most mitochondrial proteins are synthesized in the cytosol and directed into the organelle; matrix proteins contain presequences that guide them through translocases in contact sites of the outer and inner membrane. In contrast, the import of many intermembrane space proteins depends on cysteine residues and the oxidoreductase Mia40. Here, we show that both import machineries can cooperate in the biogenesis of matrix proteins. Mrp10, a conserved protein of the mitochondrial ribosome, interacts with Mia40 during passage into the matrix. Mrp10 contains an unconventional proline-rich matrix-targeting sequence that renders import intermediates accessible to Mia40. Although oxidation of Mrp10 is not essential for its function in mitochondrial translation, the disulfide bonds prevent proteolytic degradation of Mrp10 and thereby counteract instability of the mitochondrial genome. The unconventional import pathway of Mrp10 is presumably part of a quality-control circle that connects mitochondrial ribosome biogenesis to the functionality of the mitochondrial disulfide relay.

INTRODUCTION

Mitochondrial proteins are of dual genetic origin. Although the vast majority is synthesized in the cytosol and imported into mitochondria, a small number of mainly hydrophobic membrane proteins are encoded by the mitochondrial genome and synthesized by mitochondrial ribosomes. Mitochondrial ribosomes are derived from bacterial ribosomes but changed considerably during evolution (O'Brien, 2002). They acquired a number of additional, mitochondria-specific proteins and, in many cases, reduced their RNA content. It is not well understood why so many additional proteins were added, but it appears likely that the need to regulate mitochondrial protein synthesis contributed to the development of additional factors (O'Brien, 2002).

The ~1,000 different mitochondrial proteins that are nuclear encoded and synthesized on cytosolic ribosomes contain targeting signals that direct them to their specific mitochondrial subcompartments (for review, see Chacinska et al., 2009; Endo and Yamano, 2009; Neupert and Herrmann, 2007). Proteins of the mitochondrial matrix carry N-terminal matrix targeting sequences (MTSs, also called presequences), which are positively charged amphipathic helices that often are removed following translocation by the mitochondrial processing peptidase in the matrix (Vögtle et al., 2009). These presequences are recognized by cytosol-exposed receptors on the mitochondrial surface and threaded through protein-conducting channels in the translocases of the outer and inner mitochondrial membrane, named TOM and TIM23 complexes. During protein translocation contact sites of the membranes are formed so that both translocases come into close proximity thereby preventing the accessibility of imported proteins to the intermembrane space (IMS) (Dekker et al., 1997; Kellems et al., 1975).

Proteins of the second mitochondrial subcompartment, the IMS, often lack presequences and use internal targeting signals. In many cases, specific patterns of cysteine residues mediate the import into the IMS. The IMS-located oxidoreductase Mia40 binds to these cysteine residues during protein import and oxidizes them (Chacinska et al., 2004; Mesecke et al., 2005; Naoé et al., 2004). The energetic requirements of the Mia40-driven import reaction differ considerably from that of matrix proteins. Although protein translocation into the matrix requires the membrane potential across the inner membrane and ATP in the matrix, protein targeting into the IMS depends on the Mia40-mediated folding of imported proteins. Mia40 serves as oxidoreductase that can induce the formation of disulfide bonds in substrate proteins. Oxidation of Mia40 depends on the sulfhydryl oxidase Erv1, which is oxidized in vivo by cytochrome *c* and cytochrome *c* oxidase, thereby using oxygen as final electron acceptor (Allen et al., 2005; Bihlmaier et al., 2007; Dabir et al., 2007; Mesecke et al., 2005). Thus, although the membrane potential is not critical for the import of proteins via the Mia40 pathway, mutants lacking cytochrome *c* oxidase activity show reduced levels of oxidized Mia40 preventing efficient substrate oxidation (Bien et al., 2010; Bihlmaier et al., 2007).

Many substrates of Mia40 contain conserved patterns of four cysteine residues known as twin Cx_3C or twin Cx_9C motifs. Twin Cx_3C proteins are also called small Tim (translocase of the inner membrane of mitochondria) proteins and function in the import of hydrophobic inner membrane proteins. The functions of twin Cx_9C proteins are more heterogeneous and not well understood;

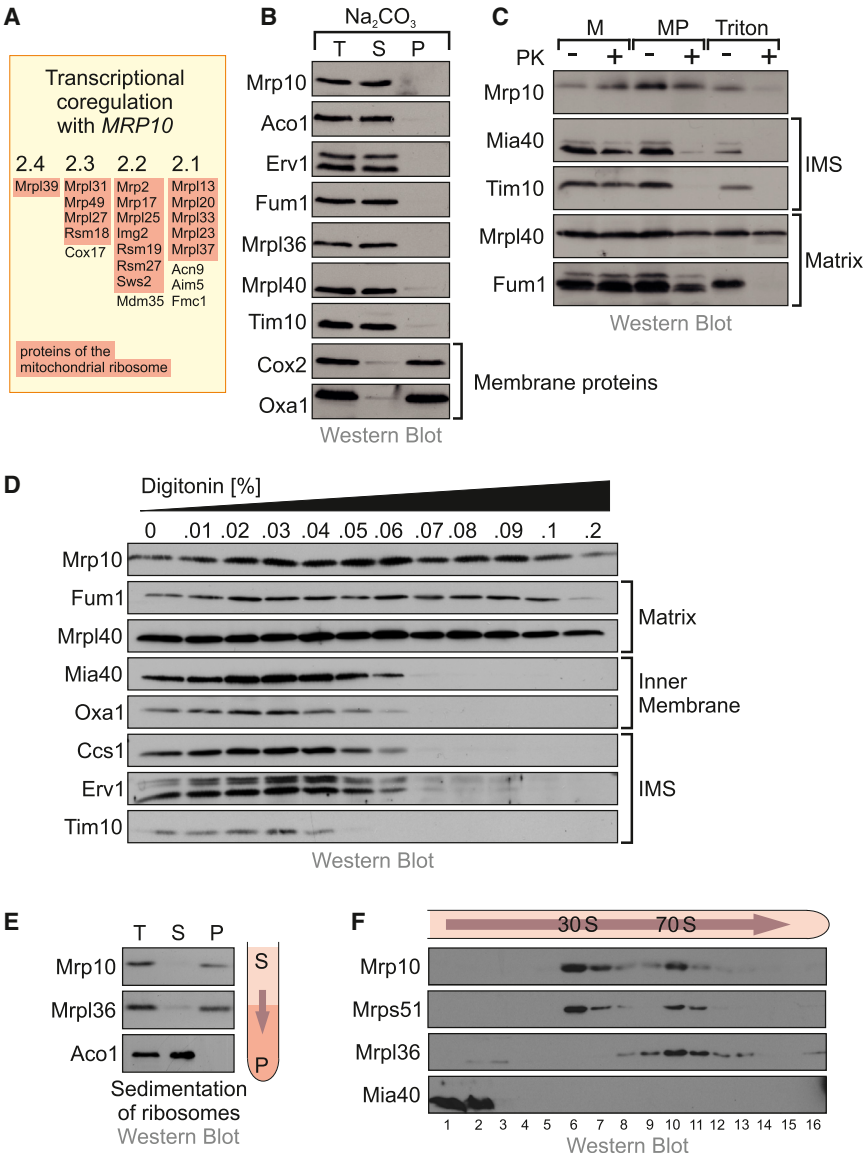

Figure 1. Mrp10 Is a Matrix-Localized Protein of the Small Subunit of the Mitochondrial Ribosome

(A) Transcript levels of Mrp10 show high coregulation scores to those of several proteins of mitochondrial ribosomes. Coregulation scores were received from the SPELL database (http://spell.yeastgenome.org/).

(B) Wild-type mitochondria were treated with Na_2CO_3 for 30 min at 4°C. Half of the sample was taken as loading control (T) and TCA precipitated. The second half was centrifuged in order to separate membrane proteins (P) from soluble proteins (S).

(C) Wild-type mitochondria were incubated in isoosmotic (M), hypoosmotic (MP), or Triton X-100-containing buffer (Triton) and treated with or without proteinase K (PK). Proteins in the respective samples were analyzed by western blotting.

(D) Wild-type mitochondria were incubated with increasing amounts of digitonin and exposed to trypsin and proteinase K.

(E) Mitoplasts were lysed in buffer containing Triton X-100. After a clarifying spin, one-half of the supernatant was taken as a loading control (T) and TCA precipitated. The second half was loaded onto a sucrose cushion and subjected to ultracentrifugation in order to separate mitochondrial ribosomes (P) from nonribosomal proteins (S).

(F) Mitochondria were lysed and ribosomes were separated on a continuous sucrose gradient. Fractions of the gradient were analyzed by western blotting.

RESULTS

Mrp10 Is a Component of the Mitochondrial Ribosome

The initial study in which *MRP10* was identified as a gene required for mitochondrial respiration (Jin et al., 1997) suggested that Mrp10 represents a component of the small subunit of the mitochondrial ribosome. This is consistent with the fact that the levels of *MRP10* transcription are tightly coregulated with those of other components of the mitochondrial ribosome (Figure 1A). According to the SPELL microarray analysis tool, 17 of the 22 gene products that show a coregulation score of larger than 2 with Mrp10 are components of the mitochondrial ribosome.

Mrp10 is a soluble mitochondrial protein (Figure 1B) that is inaccessible to protease upon hypoosmotic opening (Figure 1C) or selective digitonin lysis (Figure 1D) of the mitochondrial outer membrane, but protease-sensitive as soon as the inner membrane is opened. In these fractionation experiments, Mrp10 behaved like other matrix proteins such as fumarase (Fum1) or Mrpl40. We therefore conclude that Mrp10 is a soluble, protease-digestible protein of the mitochondrial matrix.

Mitochondrial ribosomes can be isolated from Triton X-100-lysed mitochondrial extracts by centrifugation through a high-density sucrose cushion. In these ribosomal pellet fractions, Mrp10 is found together with ribosomal proteins such as

in yeast, 14 members of this family were identified, 13 of which are also present in animals (Gabriel et al., 2007; Longen et al., 2009). Interestingly, 13 of these proteins were found to be present in the IMS, whereas one protein, Mrp10, was reported to be a component of the mitochondrial ribosome (Jin et al., 1997). Recently, also the mammalian Mrp10 homolog CHCHD1 was identified as a component of the mitochondrial ribosome (Koc et al., 2013).

In this study, we confirm that Mrp10 is a constituent of the small ribosomal subunit. Despite its final localization in the matrix, Mrp10 is a substrate of Mia40, which oxidizes Mrp10 on its transit to the matrix. Upon depletion of Mia40, the import of Mrp10 is impaired and the reduced Mrp10 that accumulates in the matrix is less stable and degraded by mitochondrial proteases. Our observations suggest that the unconventional import pathway of Mrp10 is part of a quality-control circle that connects mitochondrial ribosome biogenesis to the functionality of the mitochondrial disulfide relay.

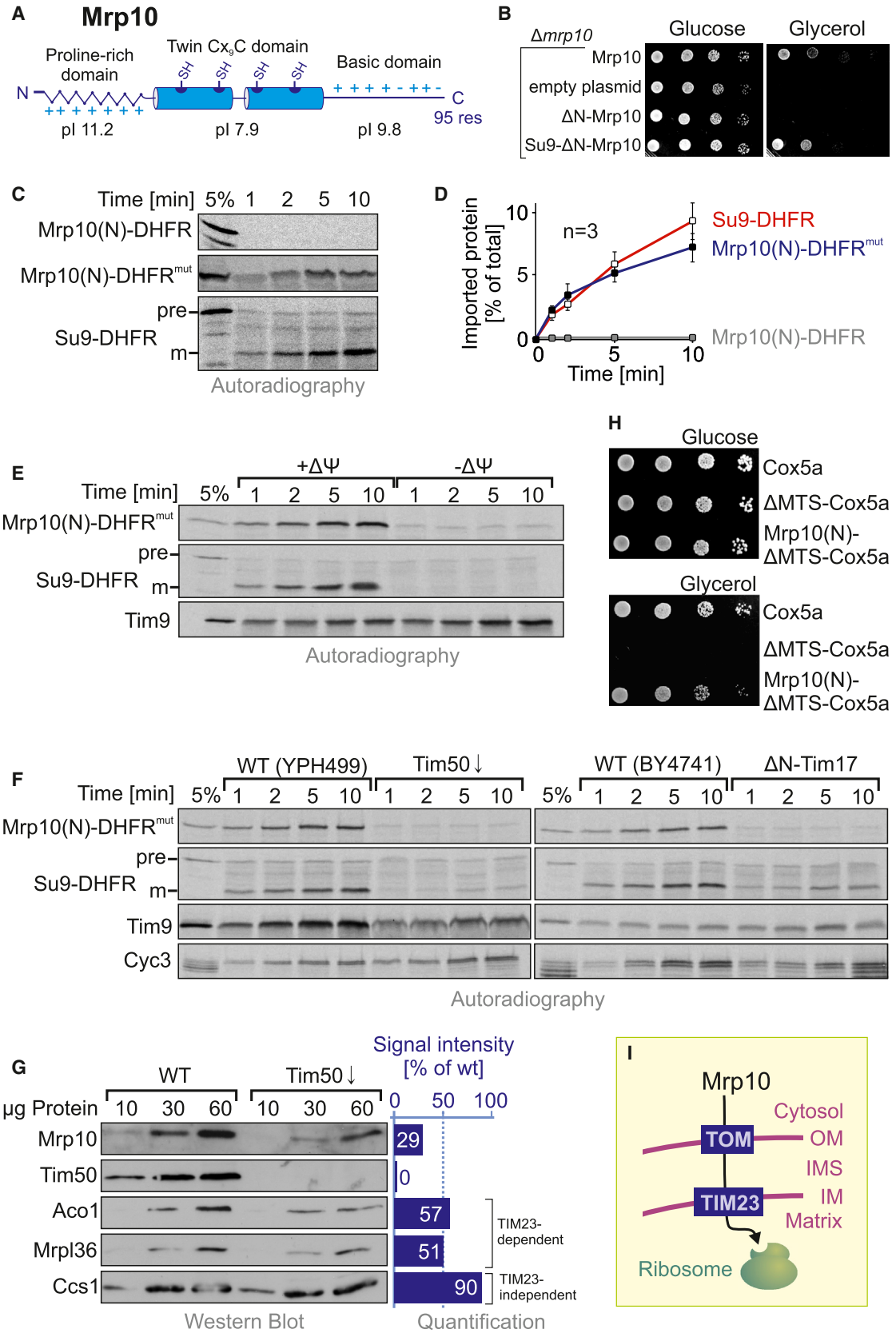

(legend on next page)

Mrpl36, whereas nonribosomal matrix proteins, such as aconitase (Aco1), remained in the supernatant (Figure 1E). When mitochondrial ribosomes were further fractionated into small and large subunits by velocity centrifugation on linear sucrose gradients, Mrp10 fractionated with the small subunit (Figure 1F, lanes 6 and 10, compare signal of small subunit protein Mrps51) and differently from proteins of the large subunit (Figure 1F, Mrpl36). We conclude that Mrp10 is a constituent of the small subunit of the mitochondrial ribosome. We have no evidence for a fraction of Mrp10 that is present in the IMS or that remained not ribosome bound in the matrix, although it is technically difficult to exclude the existence of small amounts of such species.

Mrp10 Contains an Unconventional MTS

Mrp10 is a conserved mitochondrial protein that is present in fungi, animals, plants, and most protists, but absent in bacteria (Smits et al., 2007). In all these organisms, Mrp10 consists of three characteristic regions: (1) an aminoterminal stretch of 20–45 amino acid residues that has a highly positive net charge and is rich in proline residues (Figure 2A and Figure S1 available online); (2) a central region containing a twin Cx_9C motif; and (3) a C-terminal region that is again positively charged. None of these regions show the typical features of a MTS and the TargetP algorithm predicts only a probability of 0.386 for matrix targeting (Emanuelsson et al., 2007). We tested the relevance of this region and constructed a yeast strain, which expressed an N-terminally truncated variant of Mrp10 (ΔN-Mrp10) instead of wild-type Mrp10 by plasmid shuffling to prevent the loss of mitochondrial DNA from *Δmrp10* cells. The truncated ΔN-Mrp10 protein was still found in the mitochondrial fraction but was degraded when proteases were added suggesting that the N-terminal region is critical for the translocation of Mrp10 into mitochondria (Figure S2A). In consistence, the ΔN-Mrp10 protein was neither associated with mitochondrial ribosomes (Figure S2B) nor did it restore growth of the *Δmrp10* strain on nonfermentable carbon sources (Figure 2B). However, when the well-characterized cleavable MTS of subunit 9 of the ATPase of *Neurospora crassa* ($Su9^{1-69}$) was fused to the ΔN-Mrp10 protein and the corresponding sequence was placed on a multicopy plasmid for overexpression, the *Δmrp10* mutant was rescued (Figure 2B, Su9-ΔN-Mrp10), protein synthesis in the mitochondria was restored (Figure S2C), and the levels of the mitochondrially encoded protein Cox2 were comparable to that in wild-type mitochondria (Figure S2D). From this, we conclude that the N-terminal proline-rich region of Mrp10 serves as unconventional MTS.

The Su9 presequence targets proteins to the matrix via the TIM23 translocase suggesting that the translocation pore in the TIM23 complex facilitated the import of Mrp10 at least in the context of the Su9-ΔN-Mrp10 fusion protein. In order to test whether the N-terminal region of Mrp10 is able to mediate TIM23-dependent protein import into the matrix, we generated fusion proteins of the N-terminal 29 residues of Mrp10 with mouse dihydrofolate reductase (DHFR) or a nonfolded variant of DHFR ($DHFR^{mut}$) (Vestweber and Schatz, 1988). Whereas the folded Mrp10(N)-DHFR protein was not imported into the matrix, Mrp10(N)-$DHFR^{mut}$ was efficiently transported into the matrix and reached a protease-inaccessible location (Figures 2C and 2E). Import of Mrp10(N)-$DHFR^{mut}$ was dependent on the membrane potential (Figure 2E) and the functionality of the TIM23 translocase (Figure 2F). Moreover, when the TIM23 subunit Tim50 was depleted from yeast cells we found a concomitant reduction of Mrp10 along with the reduction of other TIM23 substrates (Figure 2G).

The ability of the proline-rich domain of Mrp10 to serve as MTS was finally confirmed by a reverse complementation experiment: we used the inner membrane protein Cox5a, which has a canonical MTS for TIM23-mediated import that was experimentally characterized before (van der Laan et al., 2006; Vögtle et al., 2009). Truncation of the MTS of Cox5a results in a respiration-incompetent strain, which was rescued as soon as the mature part of Cox5a was fused to the proline-rich domain of Mrp10 (Figure 2H). In summary, we conclude that the proline-rich domain of Mrp10 serves as an unconventional MTS, which can direct proteins into the mitochondrial matrix in a membrane potential- and TIM23-dependent manner (Figure 2I).

Mrp10 Is a Substrate of Mia40

Mrp10 contains a twin Cx_9C motif found in many substrates of Mia40 (Gabriel et al., 2007; Longen et al., 2009) (Figure S1). We therefore tested whether Mrp10 can serve as a substrate of Mia40. Mia40-mediated protein oxidation can be analyzed in alkylation assays that rely on the accessibility of reduced, but not oxidized, thiol residues to alkylating reagents like 4-acetamido-4′-maleimidylstilbene-2,2′-disulfonic acid (AMS)

Figure 2. Mrp10 Contains an Unconventional Matrix-Targeting Sequence

(A) Schematic overview of the Mrp10 sequence. Charges, cysteine residues (SH), and pI values are indicated. See also Figure S1.

(B) Cells of the indicated strains were grown to log phase. Ten-fold serial dilutions were spotted on plates containing either glucose or glycerol as carbon source, and the plates were incubated at 30°C for 2 or 4 days, respectively.

(C) The depicted proteins were synthesized in reticulocyte lysate in the presence of ^{35}S-methionine and incubated for the indicated time periods with wild-type mitochondria. Nonimported material was removed by treatment with proteinase K and trypsin (100 μg/ml each). Samples were subjected to SDS-PAGE and autoradiography. 5%, 5% of radiolabeled protein used per time point; pre, precursor; m, mature form.

(D) The experiment described in (C) was repeated three times and quantified. Error bars show SDs.

(E) The depicted radiolabeled proteins were imported for the indicated time periods in wild-type mitochondria in the absence (+ΔΨ) or presence (−ΔΨ) of valinomycin, oligomycin, and antimycin A and further treated as in (C).

(F) The import reaction described in (C) was carried out with mitochondria in which Tim50 was depleted (Tim50↓) or which contained an N-terminally truncated version of Tim17 (ΔN-Tim17) (Meier et al., 2005). For comparison, the corresponding wild-type strains were used. Tim9 and Cyc3 are IMS proteins that are imported into mitochondria in a TIM23-independent manner.

(G) Increasing protein amounts of wild-type and Tim50-depleted mitochondria were analyzed by western blotting and quantified.

(H) Cells of the indicated strains were grown to log phase and growth was analyzed as described in (B).

(I) Scheme of Mrp10 import into the matrix. OM, outer membrane; IM, inner membrane.

See also Figures S1 and S2.

or methyl-polyethylenglycol-maleimide (mmPEG24) both causing gel shifts of defined sizes (Figure S3A). First, we incubated radiolabeled Cox19, a well-characterized twin Cx_9C protein, with purified Mia40 or with a $Mia40^{SPS}$ mutant that lacks the two redox-active cysteine residues (Figure S3B). Reduced, nonmodified Cox19 migrated at 12 kDa and was shifted to 14 kDa after incubation with AMS, which adds 0.5 kDa to each of the four cysteine residues of Cox19 (Figure S3B, lanes 1 and 2). Even after prolonged incubation with $Mia40^{SPS}$, Cox19 remained reduced. In contrast, when Cox19 was incubated with Mia40 its cysteines became inaccessible to AMS and the protein migrated at 12 kDa (Figure S3B, lanes 9–14). Thus, Cox19 was completely oxidized within a few minutes of incubation.

Then, we tested the oxidation of Mrp10 by purified Mia40 (Figures S3C and S3D). Whereas Mrp10 remained reduced in the presence of $Mia40^{SPS}$, it was partially oxidized as soon as it was incubated with Mia40. In the presence of Mia40, Mrp10 was rapidly converted to a semioxidized intermediate containing one disulfide bond (Figures S3C and S3D, asterisks), which over time was converted to a fully oxidized species (Figures S3C and S3D, ox.). These results indicate that in vitro Mia40 recognizes Mrp10 as a substrate protein and introduces two intramolecular disulfide bonds.

Mrp10 Interacts with Mia40 in Mitochondria

Next, we tested whether Mrp10 also interacts with Mia40 during its import into mitochondria. To this end, radiolabeled Mrp10 was imported into isolated mitochondria, which were lysed under denaturing conditions and used for immunoprecipitation with antibodies against Mia40 or with preimmune serum (Figure 3A). Thereby a disulfide-linked conjugate of Mia40 and Mrp10 was revealed, which accumulated only transiently during the initial 2 min of the import reaction (Figure 3B). Mrp10 was released from this mixed disulfide when the immunoprecipitate was treated with DTT (Figure S3E). Peptide scan experiments suggest that Mia40 binds in addition to the MISS/ITS-like signal to terminal regions of Mrp10 (Figure S3F).

The presence of glutathione concentrations larger than 10 mM reduced the import efficiency of Mrp10 similarly to what is observed for IMS proteins that are imported in a Mia40-dependent manner (Figure 3C) (Bien et al., 2010; Mesecke et al., 2005). Under these conditions, the CPC motif in Mia40 is largely reduced and the oxidation of imported proteins therefore less efficient. Interestingly, glutathione also resulted in a strongly accelerated degradation of already imported Mrp10 (Figure 3D). This suggests that oxidation of Mrp10 is critical for its stable accumulation in mitochondria.

The relevance of Mia40 for the biogenesis of Mrp10 was also obvious from the observation that the endogenous levels of Mrp10 were dependent on the levels of Mia40 so that up- or downregulation of Mia40 resulted in increased or decreased amounts of Mrp10, respectively (Figure 3E). However, it should be noted that the reduction of Mrp10 in Mia40-depleted mitochondria was not as pronounced as that of the Mia40-dependent IMS proteins Ccs1 and Erv1. Mrp10 levels were not decreased in Erv1-depleted mitochondria (Figure 3F). This is reminiscent to the import of the IMS protein Atp23 for which the binding to Mia40 rather than the Mia40-mediated cysteine oxidation is critical for the import reaction (Weckbecker et al., 2012). However, this experiment does not exclude a role for Erv1 in Mrp10 biogenesis. Also, the levels of Mia40 were not reduced in Erv1-depleted cells (Figure 3F), although Erv1 plays an important role in the formation of the disulfide bonds in Mia40 (Chatzi et al., 2013).

The relevance of Mia40 for Mrp10 biogenesis might suggest that its oxidation is required. We therefore tested the redox state of Mrp10 at steady-state levels in extracts of cells or isolated mitochondria. The samples were treated with trichloroacetic acid (TCA) to preserve the redox state of thiols because acidic conditions prevent the formation of the reactive thiolate anion. Subsequently, proteins were denatured with SDS and treated either with N-ethylmaleimide (NEM) to block thiol groups, with tris(2-carboxyethyl)phosphine (TCEP) to reduce disulfide bonds and/or with AMS and mmPEG24 (Bien et al., 2010). As shown in Figure 3G, the size of Mrp10 was only shifted by these reagents when the protein samples were treated with TCEP but not if they were exposed to alkylating reagents directly. From this, we conclude that endogenous Mrp10 is fully oxidized in vivo.

In summary, we conclude that Mrp10 is a matrix protein that transiently interacts with Mia40 during its translocation through the IMS (Figure 3H) and ends up as a subunit on mitochondrial ribosomes that contains two structural disulfide bonds. The interaction of the protein with Mia40 thereby was surprising, given the fact that previous studies had shown that matrix proteins are transported through tightly connected TOM and TIM23 translocases so that their access to proteins of the IMS is restricted (Chacinska et al., 2003).

Oxidized Mrp10 Can Be Imported into the Mitochondrial Matrix

The oxidation of a matrix protein in the mitochondrial IMS was completely unexpected and inspired us to test the effect of preoxidation of the Mrp10 protein prior to the import experiment. To this end, we treated Mrp10 with diamide, a compound that induces disulfide bond formation. In the absence of diamide, Mrp10 was reduced and the addition of the alkylating reagent mmPEG24 caused a characteristic size shift (Figure 4A, upper panel, arrowhead). In contrast, when Mrp10 was pretreated with diamide, mmPEG24 did not modify the protein unless it was reduced again by addition of TCEP (Figure 4A, lower panel, arrowhead). However, when mitochondria were added to these proteins, both the reduced and the oxidized forms of Mrp10 were imported with comparable efficiencies. From this, we conclude that the formation of intramolecular disulfide bonds does not prevent translocation of Mrp10 across the inner membrane.

To analyze productive matrix transport of Mrp10 by an alternative approach, we developed an in vitro assay in which the assembly of Mrp10 into ribosomes was followed. To this end, we isolated mitochondria that contained or lacked endogenous Mrp10 by use of a strain in which the only copy of the *MRP10* gene was under control of a tet promoter. Radiolabeled Mrp10 was imported into these mitochondria and nonimported material was removed by protease treatment before ribosomes were purified. More than half of the imported radiolabeled Mrp10 was found in the ribosomal pellet when Mrp10-depleted mitochondria were used, whereas much lower levels assembled into ribosomes when Mrp10 was overexpressed (Figure 4B, compare

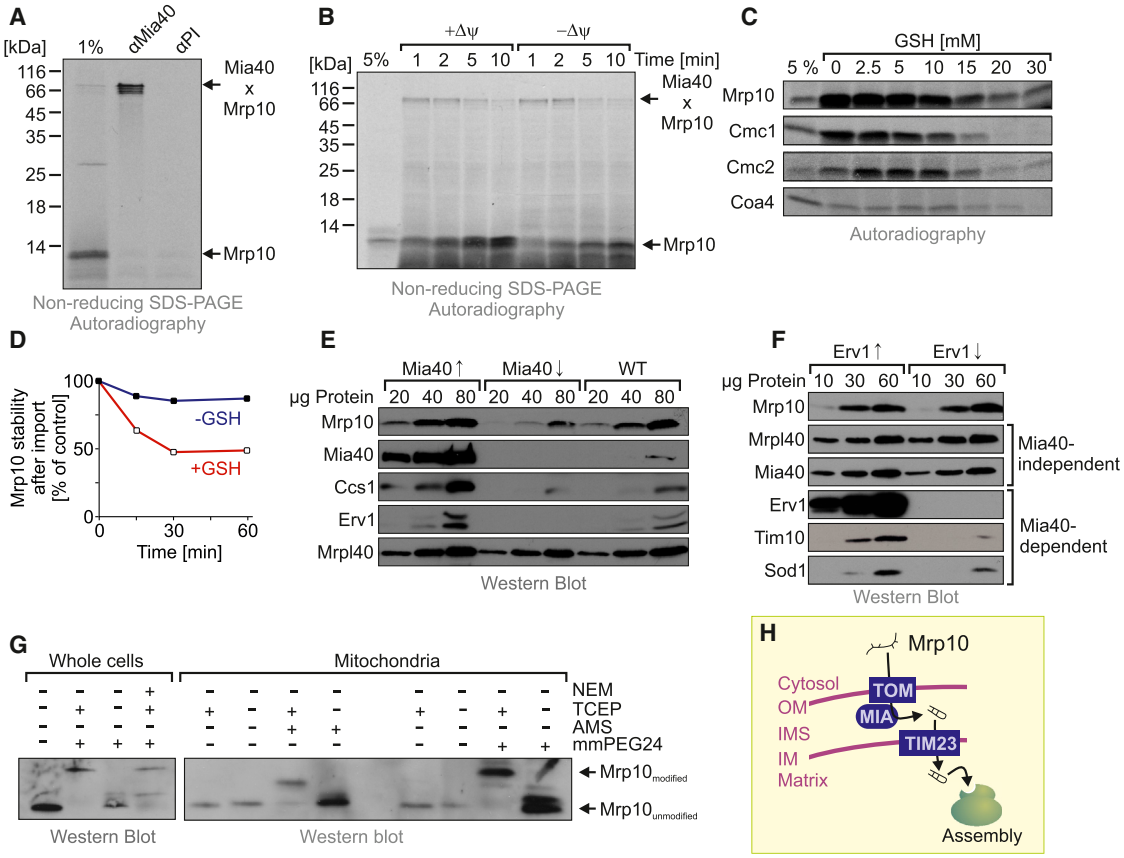

Figure 3. Mrp10 Is Oxidized by Mia40 during Its Import into Mitochondria

(A) Radiolabeled Mrp10 was imported in Mia40-overexpressing mitochondria. After addition of 50 mM NEM the Mia40-Mrp10 intermediate was isolated by immunoprecipitation using Mia40 antibodies (αMia40). The samples were subjected to nonreducing SDS-PAGE and autoradiography. 1%, 1% of the total amount used in the assay; αPI, preimmune serum.

(B) Radioactively labeled Mrp10 was imported in mitochondria in the absence (+ΔΨ) or presence (−ΔΨ) of valinomycin, oligomycin, and antimycin A, and the samples were subjected to nonreducing SDS-PAGE and autoradiography.

(C) Protein import of the depicted proteins into isolated wild-type mitochondria in the presence of different amounts of reduced glutathione (GSH) for 8 min at 25°C was analyzed as described in (B).

(D) Radioactively labeled Mrp10 was imported for 15 min into mitochondria in the presence of 0 or 30 mM GSH. The import reaction was stopped by centrifugation; mitochondria were resuspended in import buffer without or with GSH and further incubated at 25°C. The levels of imported Mrp10 during the postincubation period were quantified. Shown are the levels of imported proteins at different postincubation times in comparison to the levels at the beginning of the chase reaction.

(E and F) Protein levels in mitochondria isolated from designated strains were analyzed by western blotting.

(G) The redox state of endogenous Mrp10 was analyzed in whole cells or isolated mitochondria after TCA-precipiation by use of the alkylating reagents mmPEG24 and AMS.

(H) Schematic representation of the role of Mia40 during Mrp10 import.

See also Figure S3.

totals, T, to ribosomal pellet fractions, P). When Mrp10 was imported into *rho*^{0} mitochondria that lack ribosomes, considerably lower amounts of Mrp10 were found in the pellet fraction (Figure S4A) confirming that the detection of Mrp10 indeed reflected its association with ribosomes. We then used this assay to monitor the assembly of imported preoxidized Mrp10 into ribosomes: Mrp10 was preoxidized with diamide and incubated with mitochondria or mitoplasts before ribosomes were prepared. As shown in Figure 4C, most of the imported Mrp10 was coisolated with ribosomes (arrowheads). From this, we conclude that oxidized Mrp10 is able to translocate across the inner membrane and to assemble into the mitochondrial ribosome.

The Cysteine Residues Are Dispensable for the Import of Mrp10

The import mechanism of several twin Cx_3C and twin Cx_9C proteins (Cox17, Cox19, Tim9, Tim10, and Tim13) was studied previously and—at least in the in vitro experiments used—for all these proteins the cysteine residues were found to be critical for the rate or efficiency of mitochondrial import (Curran et al., 2002; Mesecke et al., 2005; Milenkovic et al., 2009; Sideris et al., 2009; Sideris and Tokatlidis, 2007). Therefore, we tested whether the cysteines were similarly critical for the import of Mrp10. We generated a variant of Mrp10 in which all four cysteine residues were replaced by serine residues (Figure 5A). This Mrp10C1234S protein was still

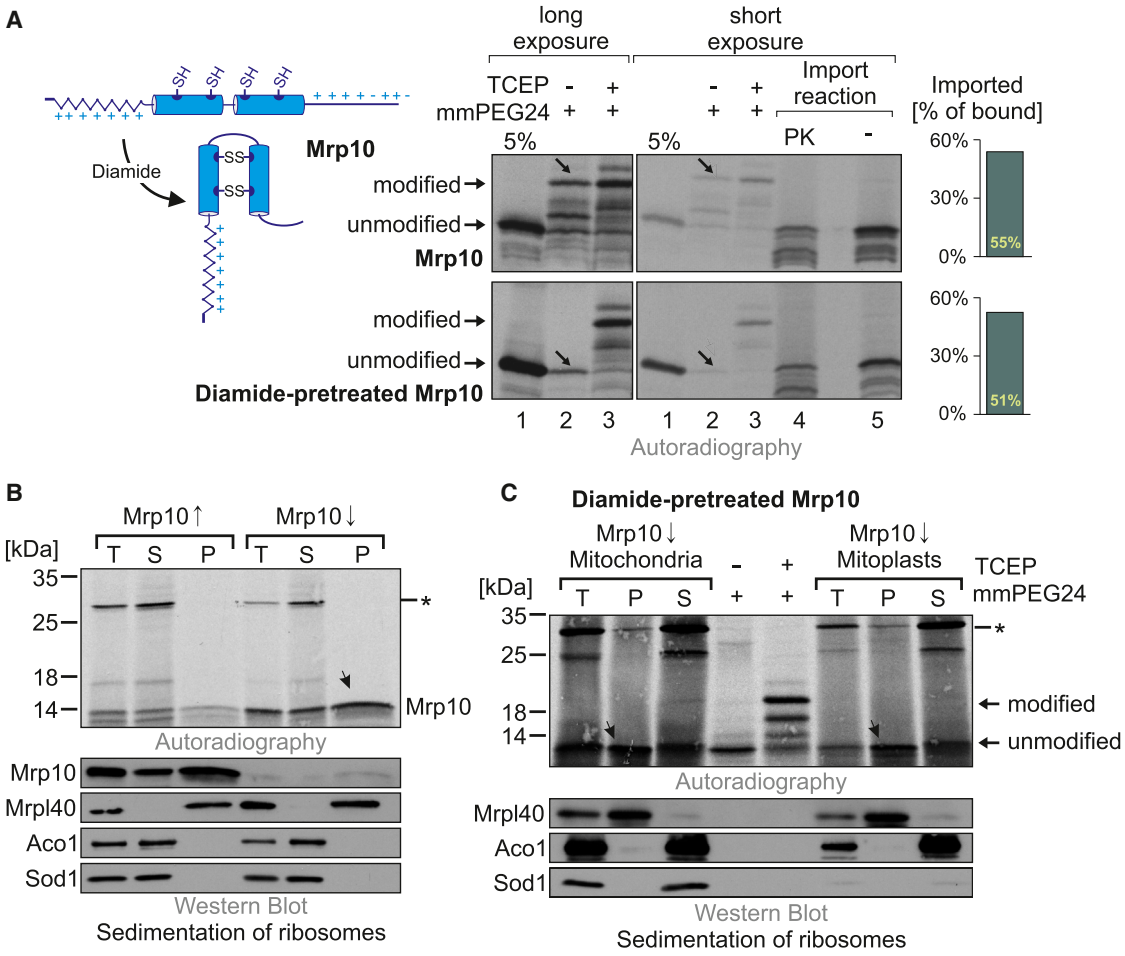

Figure 4. Oxidized Mrp10 Can Be Imported into the Matrix

(A) Radiolabeled Mrp10 was pretreated in the absence or presence of diamide, which induces cysteine oxidation. The reduced or oxidized redox states of Mrp10 were verified by alkylation with mmPEG24 (lane 2, arrowheads). When thiols in the protein were initially reduced with TCEP, all cysteines were accessible to mmPEG24 (lane 3). Diamide was quenched and Mrp10 was incubated with isolated mitochondria. Mitochondria-bound and protease-resistant Mrp10 (PK) levels were visualized by autoradiography and quantified.

(B) Radiolabeled Mrp10 was imported into isolated mitochondria of cells in which Mrp10 was overexpressed or depleted, respectively. After the import, mitochondria were lysed, and the extracts were subjected to ultracentrifugation in order to isolate the ribosomes (P) as described in Figure 1E. The asterisk depicts a background signal of a protein in the supernatant (S) that does not associate with ribosomes. Fractionation was controlled by western blotting.

(C) Mrp10 was oxidized by diamide pretreatment and imported into mitochondria before its association with ribosomes was tested. Note that oxidized Mrp10 is efficiently imported and assembles into mitochondrial ribosomes.

efficiently imported into mitochondria (Figure 5B). In contrast to the IMS protein Tim9, Mrp10C1234S was resistant to protease even when the outer membrane was lysed with digitonin, indicating that Mrp10C1234S, like Mrp10, was imported into the matrix. The overall efficiency of protein import was similar to that of Mrp10 and still strongly accelerated in the presence of Mia40 (Figures 5C and 5D). Hence, Mia40 obviously stimulates the overall import of Mrp10 in an oxidation-independent reaction, similar to what was observed before with other Mia40 substrates such as Atp23 (Weckbecker et al., 2012).

In the case of Atp23, it was found that cysteine residues were not critical for protein import per se but important to prevent proteolytic degradation of the protein in mitochondria. We therefore tested the relevance of the cysteine residues in Mrp10 in vivo. When Mrp10C1234S was overexpressed from a multicopy plasmid under control of the strong triosephosphate isomerase promoter, the protein accumulated in the mitochondria at similar levels as the wild-type protein (Figure S4B), allowed growth on nonfermentable carbon source (Figure 5F), assembled into the mitochondrial ribosomes and facilitated mitochondrial protein synthesis (Figure S4C). Hence, Mrp10C1234S was able to functionally replace Mrp10. In contrast, when Mrp10C1234S was expressed under control of the *MRP10* promoter from a single-copy plasmid, we observed reduced growth on nonfermentable carbon sources (Figure 5F), a considerably decreased stability of the mitochondrial genome (Figure 5E) and reduced steady-state levels of Mrp10 (Figure 5G), which was particularly pronounced at higher temperature. Genome instability is associated with many mutants of ribosomal proteins including Mrp10 (Merz and Westermann, 2009).

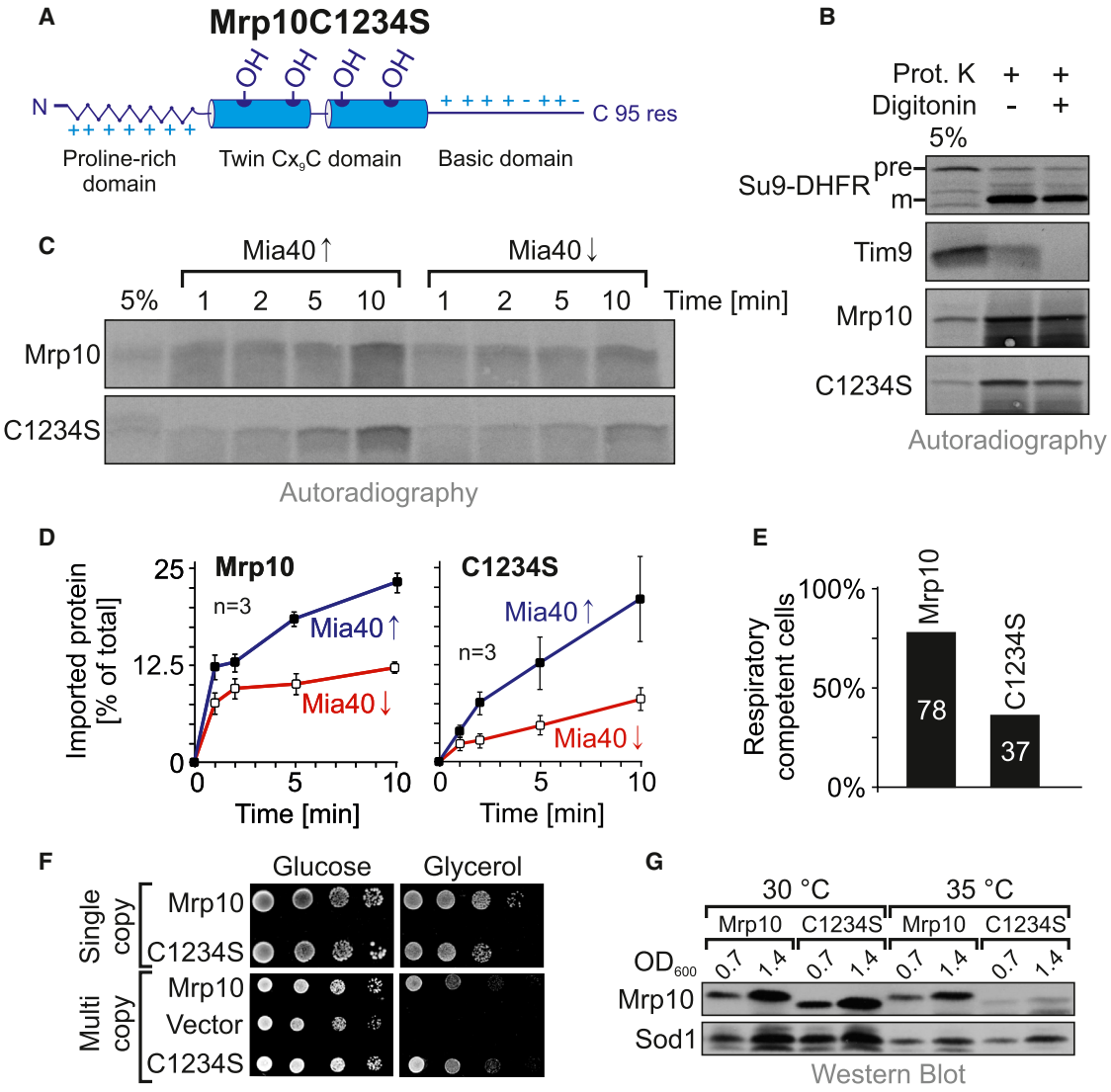

Figure 5. The Cysteine Residues of Mrp10 Are Not Essential for Protein Import

(A) Scheme of the cysteineless variant of Mrp10. OH depicts serine residues that replace cysteines.

(B) The depicted proteins were radioactively labeled and imported into mitochondria. After the import reaction the mitochondria were treated with 0.06% digitonin in order to selectively disrupt the outer membrane before proteinase K (PK) was added.

(C) Radioactively labeled Mrp10 or Mrp10C1234S (C1234S) was imported into mitochondria that were isolated from cells in which Mia40 was up- or down-regulated.

(D) The experiments shown in (C) were carried out three times and quantified. The amounts of imported protein were related to the total amount of radiolabeled protein used per sample. Error bars show SDs.

(E) Cells transformed with single-copy plasmids expressing Mrp10 and Mrp10C1234S under the control of the endogenous Mrp10 promoter were grown on glucose-containing minimal medium at 37°C. The number of respiration-competent (*rho*$^+$) cells in each sample was analyzed by plating aliquots of the cultures onto YPD and YPG plates. The graph depicts the number of cells that remained respiration-competent during a time period of 24 hr.

(F) Overexpression of Mrp10C1234S confers growth on nonfermentable carbon source, whereas expression of the protein from single-copy plasmids resulted in reduced growth on glycerol.

(G) Cells expressing Mrp10 or Mrp10C1234S from a single-copy plasmid were incubated for 3 days in selective glycerol-containing medium at the indicated temperatures. Proteins were extracted from equal amounts of cells and analyzed by western blotting.

See also Figure S4.

The Cysteine Residues in Mrp10 Stabilize Mrp10 In Vivo

To assess the stability of Mrp10 and Mrp10C1234S more directly, we expressed both proteins from a controllable tet promoter in a strain in which the chromosomal *MRP10* gene was deleted. Upon repression of the tet promoter by addition of doxycycline, the degradation of Mrp10 and Mrp10C1234S was followed by western blotting over time (Figures 6A and 6B). Whereas Mrp10 remained relatively stable over several hours, Mrp10C1234S was rapidly degraded, and after about 2 hr almost no Mrp10C1234S was detectable anymore. It should be taken in

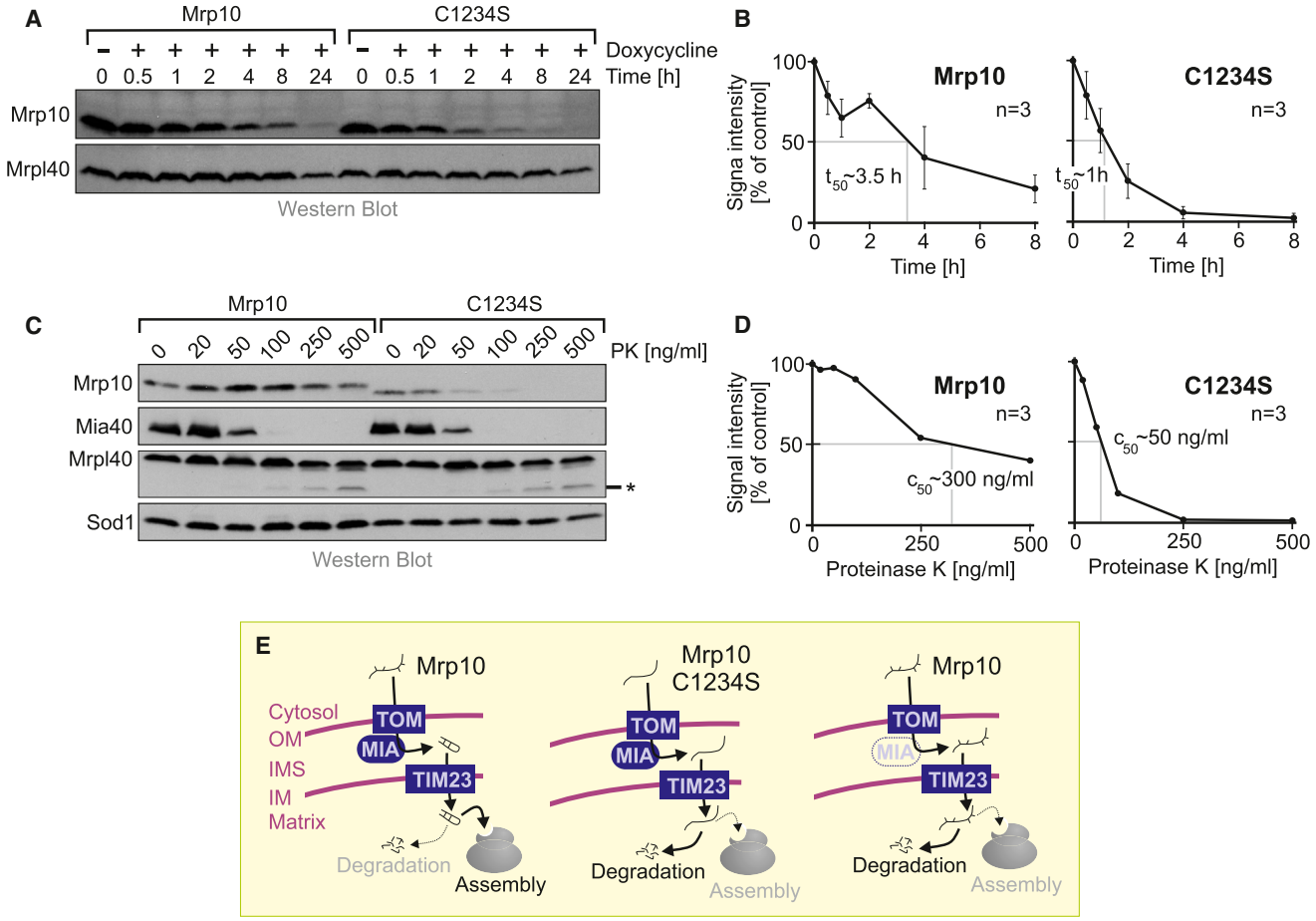

Figure 6. The Cysteine Residues in Mrp10 Contribute to Its Proteolytic Stability

(A) Yeast cells in which the expression of Mrp10 and Mrp10C1234S was under the control of a tetracycline promoter were incubated with 20 μg/ml doxycycline. After the indicated time points, samples were taken and TCA precipitated. The samples were subjected to SDS-PAGE and western blotting.

(B) The experiment shown in (A) was repeated three times and quantified. Mean values and SDs are shown.

(C) Mitochondria containing Mrp10 or Mrp10C1234S were lysed in Triton X-100-containing buffer and exposed to increasing amounts of PK. The proteins in these samples were TCA-precipitated and analyzed by western blotting.

(D) The experiment shown in (C) was repeated three times and quantified. Mean values are shown.

(E) Schematic representation of the Mia40-mediated import of Mrp10. In the absence of cysteine residues in its sequence or in the absence of Mia40, Mrp10 is still imported and can associate with ribosomes. However, under these conditions Mrp10 is less stable and partially degraded.

See also Figure S5.

consideration that the actual lifetime of the protein might be even lower because the *MRP10* mRNAs are depleted with a certain delay after doxycycline addition.

The contribution of cysteine residues to the inaccessibility of Mrp10 against proteases was also obvious when mitochondrial extracts were exposed to increasing concentrations of protease (Figures 6C and 6D). Whereas Mrp10 was largely resistant to up to 500 ng/ml proteinase K, Mrp10C1234S was already degraded by addition of 50 ng/ml proteinase K. From this, we conclude that the disulfide bonds in Mrp10 confer proteolytic stability to the protein.

In summary, we conclude that the cysteine residues of Mrp10 are neither essential for its translocation into the matrix nor for its assembly into ribosomes. However, the cysteine residues in Mrp10 still have a functional relevance as they presumably contribute to the stability of the protein (Figure 6E).

The Stability of Mrp10 Depends on the Activity of the Respiratory Chain

Next, we tested the stability of oxidized and reduced species of Mrp10 in whole cells. To this end, we developed a pulse-chase labeling assay in which newly synthesized proteins were radiolabeled with ^{35}S-methionine in logarithmically growing yeast cells for 10 min. Labeling was stopped by the addition of an excess of unlabeled methionine. After different time periods, aliquots were removed, cells were precipitated with TCA and the samples were treated with alkylating reagents to monitor the redox state of cysteine thiols. Finally Mrp10 was isolated from these samples by immunoprecipitation and visualized by autoradiography. First, we verified that this assay reflects the Mia40-mediated oxidation of Mrp10. As shown in Figure 7A, after the labeling period of 10 min, a significant fraction of the synthesized Mrp10 was accessible to mmPEG24 (i.e., reduced), whereas

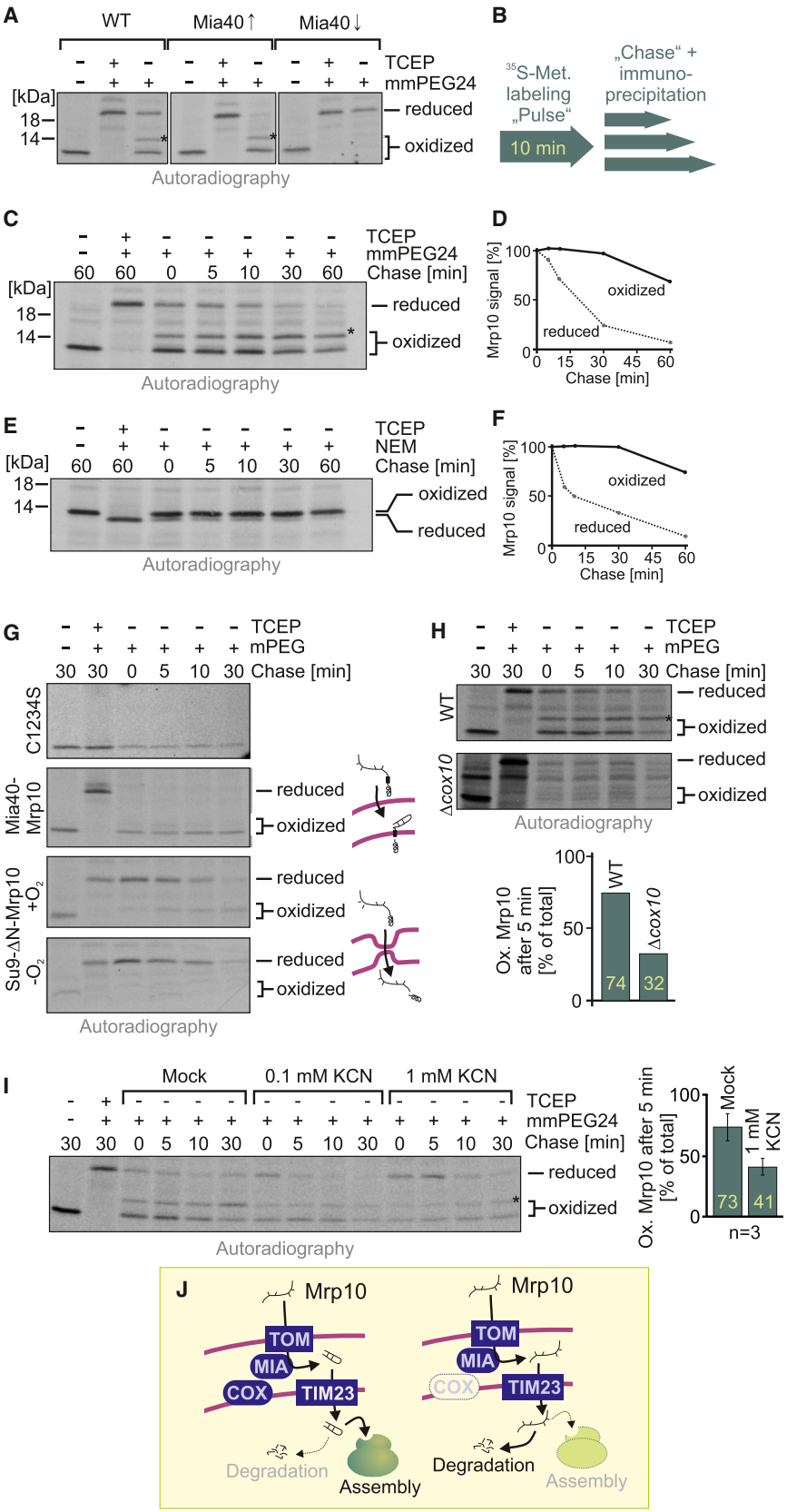

Figure 7. Mia40 and Cytochrome *c* Oxidase Activity Influence Mrp10 Stability In Vivo

(A) Wild-type (WT) cells or strains in which Mia40 was up- or downregulated were radiolabeled by the addition ^{35}S-methionine for 10 min, and the redox state of Mrp10 was analyzed by an alkylation assay using mmPEG24. The asterisk contains a partially oxidized species of Mrp10 in which one disulfide bond is opened, presumably due to the reducing conditions in the matrix.

(B–D) Mrp10 was assessed by pulse labeling as described in (A). Stability of the different redox species of Mrp10 was followed during post-incubation periods (chase) and quantified.

(E and F) The stability of reduced and oxidized Mrp10 was followed on nonreducing SDS gels after NEM treatment and quantified.

(G) Cells expressing Mrp10C1234S, Mia40-Mrp10, or Su9-ΔN-Mrp10 were radiolabeled for 10 min and analyzed as described in (C). For the samples shown in the bottom panel, the cells were incubated in a hypoxia chamber to prevent oxidation by atmospheric oxygen.

(H) Mrp10 oxidation was analyzed in wild-type or a cytochrome *c* oxidase (*Δcox10*) mutant as described for (C) and quantified.

(I) Inhibition of cytochrome *c* oxidase by potassium cyanide (KCN) impairs Mrp10 oxidation. KCN was added to the cells 60 min prior to the labeling period, and the samples were further treated as in (C). Mean values and SDs are shown.

(J) Hypothetical model to illustrate the relevance of cytochrome *c* oxidase (COX) for oxidation and stability of Mrp10. See Discussion for detail.

the rest was inaccessible (i.e., oxidized). When Mia40 was overexpressed, almost all Mrp10 was oxidized, and, on the contrary, Mrp10 remained reduced when Mia40 was depleted. From this, we conclude that this assay monitors the oxidation of Mrp10 in whole cells under physiological growth conditions. Obviously, the activity of Mia40 is limiting for Mrp10 oxidation.

Next, we followed the stability of oxidized and reduced forms of Mrp10 after 10 min labeling during postlabeling chase periods (Figure 7B). Whereas the oxidized species of Mrp10 remained rather constant, the reduced form of Mrp10 rapidly disappeared (Figures 7C and 7D). Because the import through the IMS and the interaction with Mia40 occurs mainly within 2 min (Figure 3B), we assume that the reduction of the signals is mainly due to protein degradation rather than due to oxidation of the reduced species. However, we cannot formally exclude some oxidation of Mrp10 during the chase period. Thus, the in vivo assay also indicates a profound instability of the reduced Mrp10 species, which is consistent with our observations with purified Mrp10 protein or isolated mitochondria.

Reduced and oxidized species of Mrp10 can also be distinguished on nonreducing SDS gels without the use of bulky alkylating reagents (Figure 7E). When the stability of both species were followed using these gels, again the reduced Mrp10 was found to be much faster degraded than the oxidized form (Figure 7F).

The strong impact of the oxidation of Mrp10 on its stability was further evident from experiments in which we altered the N-terminal targeting signal of the protein (Figure 7G). When the stop-transfer signal of Mia40 was used to direct Mrp10 into the IMS, all of this fusion protein was efficiently oxidized and remained stable. In contrast, when the Su9 presequence mediated the import into the matrix, Mrp10 was not efficiently oxidized, particularly under anaerobic conditions, and hence, was proteolytically unstable.

Because we found that the redox state of imported Mrp10 strongly depends on the Mia40 activity, we tested the influence of components that play a role in the biogenesis of Mia40 substrates. Oxidation of Mrp10 was particularly affected in the absence of cytochrome *c* oxidase, the enzyme required for reoxidation of Mia40 (Bihlmaier et al., 2007; Dabir et al., 2007) (Figure 7H). The relevance of cytochrome *c* oxidase activity was also confirmed when enzyme inhibitors were used. Although inhibition of cytochrome *c* reductase with antimycin A did not affect Mrp10 oxidation (not shown), inhibition of cytochrome *c* oxidase with cyanide almost completely prevented the oxidation of Mrp10 (Figure 7I). In summary, we observed that oxidation of Mrp10 depends on the mitochondrial redox relay and on the functionality of cytochrome *c* oxidase and strongly influences the stability of the newly imported protein in vivo.

DISCUSSION

Our results demonstrate that Mrp10 uses an unconventional import pathway that differs from the import of other matrix proteins in several respects: (1) The N terminus of Mrp10 serves as matrix-targeting signal, but, whereas proline residues are typically absent from MTSs of other matrix proteins (Vögtle et al., 2009), 25% of the amino acid residues in the N terminus of yeast Mrp10 are proline residues. Similarly high proline concentrations are present in Mrp10 homologs of other organisms (Figure S1). It appears conceivable that Mrp10 employs its unconventional proline-rich targeting sequence in order to prevent the close tethering of TOM and TIM23 complexes in contact sites to improve the access of import intermediates of Mrp10 to the disulfide relay in the IMS. (2) The MTS of Mrp10 is not processed by the matrix processing peptidase and is part of the mature protein. However, the N-terminal region is not critical for Mrp10 function because its replacement by the Su9 presequence, which is removed in the matrix, leads to a functional ΔN-Mrp10 protein. (3) Mrp10 contains four conserved cysteine residues, which are oxidized by Mia40 during the import reaction. Whereas other Mia40 substrates that were analyzed so far are efficiently oxidized during import (Bien et al., 2010; Curran et al., 2002; Sideris and Tokatlidis, 2007), only about half of the imported Mrp10 is oxidized. The degree of Mrp10 oxidation thereby depends on the activity of cytochrome *c* oxidase, which serves as terminal component in the mitochondrial disulfide relay (Bihlmaier et al., 2007; Dabir et al., 2007). (4) Despite the presence of two disulfide bonds in its structure, Mrp10 is translocated across the inner membrane. This was unexpected but it was reported before that the formation of disulfide bonds in fusion proteins does not prevent their import into the matrix (Huang et al., 2002). Moreover, it was previously shown that the translocation pore of the TIM23 channel can transport loop structures of proteins such as the one in the internal targeting signals of Bcs1 or Tim14/Pam18 (D'Silva et al., 2003; Fölsch et al., 1996). The diameter of oxidized Mrp10 might be similar to that of these TIM23 substrates. (5) The matrix protein Mrp10 is oxidized at steady-state levels, whereas thiol residues in matrix proteins are assumed to be generally reduced due to the presence of mitochondrial glutaredoxin and thioredoxin systems (Hu et al., 2008; Kojer et al., 2012). Interestingly, we observed in the pulse-chase experiments shown in Figure 7 that two oxidized Mrp10 species are present. Initially, a completely oxidized form is generated by Mia40, but over time a fraction of this species is slowly converted into a form that is partially accessible to alkylating reagents (Figure 7, asterisks, also visible in the western blots shown in Figure 3G). This indicates that in the matrix, a fraction of Mrp10 contains only one disulfide bond, which might reflect the activity of reducing enzymes in this compartment. However, at steady state, Mrp10 was almost exclusively found as completely oxidized protein.

Why does Mrp10 use such an unconventional import pathway? The cysteine residues in Mrp10 are highly conserved pointing at a critical function, which was preserved during more than one billion years of evolution. Nevertheless, we found that Mrp10C1234S fully complemented the deletion mutant, at least upon overexpression of the protein. However, at lower levels of expression, this variant resulted in the loss of mitochondrial DNA (mtDNA) and the ability to synthesize proteins. At present it is not entirely clear which of these symptoms is primary and which secondary, because a role in mtDNA stabilization was found for many ribosomal proteins (Merz and Westermann, 2009). In a proteome-wide expression study in yeast (Ghaemmaghami et al., 2003), Mrp10 was identified as one of the least abundant component of the mitochondrial ribosome (Figure S5).

Although these data should be interpreted with caution, they are consistent with our observation that Mrp10 was more rapidly degraded than other components of the mitochondrial ribosomes that we tested (Figure 2G; data not shown). Our observations strongly suggest that Mrp10 plays a regulatory role in mitochondrial protein expression. They are consistent with a hypothesis, which is illustrated in Figure 7J. In wild-type cells, a considerable fraction of Mrp10 is oxidized during import by Mia40 and assembles into the small subunit of the ribosomes. However, in mutants in which cytochrome *c* oxidase activity is reduced, Mrp10 is not efficiently oxidized so that a larger fraction of Mrp10 is degraded, thereby lowering mitochondrial protein expression. Such a control mechanism would be an elegant regulatory circuit that reduces the production of not properly functional cytochrome *c* oxidase subunits in cells. Cells contain many copies of mitochondrial genomes that, particularly in older cells, accumulate mutations (Larsson, 2010). In particular, cytochrome *c* oxidase is highly sensitive to these mutations, and reduced levels of complex IV were found as direct or indirect consequence of many mtDNA mutations. We therefore speculate that the depletion of Mrp10 in such mutants might help to prevent protein expression from these genomes and thereby contributes to the counterselection against mtDNA mutations. It will be exciting to assess the relevance for Mrp10 for mitochondrial fitness states in aging cells more specifically in the future.

EXPERIMENTAL PROCEDURES

Yeast Strains and Media

All yeast strains in which Mrp10 variants were used derived from the wild-type strain YPH501 after haploid spore generation and plasmid shuffling (for details, see Supplemental Experimental Procedures). The deletion strains *Δcox10* were received from the yeast deletion library based on BY4742. The ΔN-Tim17 and its corresponding wild-type BY4741 were described before (Meier et al., 2005). In order to deplete Mia40 or Tim50, strains were used in which the respective genes are under control of a *GAL10* promoter (Mesecke et al., 2005; Mokranjac et al., 2003). Protein overexpression was achieved by growing the strains in galactose-containing medium, and protein depletion was achieved by growth in glucose containing medium. All strains were grown in YP (1% yeast extract, and 2% peptone), lactate, or minimal medium with 2% glucose or galactose as carbon sources at 30°C (Altmann et al., 2007). A complete list and additional information to the yeast strains used in this study are shown in the Supplemental Experimental Procedures.

Purification of Recombinant Mia40 and Mia40^{SPS} and In Vitro Oxidation of Mrp10

The purification of recombinant Mia40 and Mia40 SPS as well as the in vitro oxidation experiment of Mrp10 were performed as described previously (Bien et al., 2010).

In Vivo Oxidation of Mrp10

In order to measure the oxidation of Mrp10 in vivo, 2 OD_{600}/ml cells per sample were harvested, washed twice in minimal medium, and resuspended in minimal medium without cysteine and methionine. 22 μCi ^{35}S-methionine was added per sample, and the cells were incubated 10 min at 30°C. Radioactive labeling was stopped by addition of nonlabeled methionine, and samples were taken after different time periods. The cells were pelleted, TCA precipitated, and the redox state of each protein sample was determined as described above. Afterward, the samples were incubated with lysis buffer (2.5% Triton X-100, 30 mM Tris [pH 8] [HCl], 100 mM NaCl) and subjected to immunoprecipitation with Mrp10-specific antibodies.

Additional information can be found in the Supplemental Experimental Procedures.

SUPPLEMENTAL INFORMATION

Supplemental Information includes Supplemental Experimental Procedures and five figures and can be found with this article online at http://dx.doi.org/10.1016/j.devcel.2013.11.007.

ACKNOWLEDGMENTS

We thank Sabine Knaus for technical assistance, Dejana Mokranjac for the *GAL-TIM50* mutant, Tom Fox for an antibody against Mrps51, Melanie Bien and Daniel Weckbecker for help with some experiments, and the Deutsche Forschungsgemeinschaft (He2803/4-2 and GRK845) and the Landesschwerpunkt für Membrantransport Rheinland-Pfalz for financial support.

Received: May 29, 2013
Revised: September 9, 2013
Accepted: November 7, 2013
Published: December 19, 2013

REFERENCES

Allen, S., Balabanidou, V., Sideris, D.P., Lisowsky, T., and Tokatlidis, K. (2005). Erv1 mediates the Mia40-dependent protein import pathway and provides a functional link to the respiratory chain by shuttling electrons to cytochrome c. J. Mol. Biol. *353*, 937–944.

Altmann, K., Dürr, M., and Westermann, B. (2007). *Saccharomyces cerevisiae* as a model organism to study mitochondrial biology. In Mitochondria Practical Protocols, D. Leister and J.M. Herrmann, eds. (Totowa, NJ: Humana Press), pp. 81–90.

Bien, M., Longen, S., Wagener, N., Chwalla, I., Herrmann, J.M., and Riemer, J. (2010). Mitochondrial disulfide bond formation is driven by intersubunit electron transfer in Erv1 and proofread by glutathione. Mol. Cell *37*, 516–528.

Bihlmaier, K., Mesecke, N., Terziyska, N., Bien, M., Hell, K., and Herrmann, J.M. (2007). The disulfide relay system of mitochondria is connected to the respiratory chain. J. Cell Biol. *179*, 389–395.

Chacinska, A., Rehling, P., Guiard, B., Frazier, A.E., Schulze-Specking, A., Pfanner, N., Voos, W., and Meisinger, C. (2003). Mitochondrial translocation contact sites: separation of dynamic and stabilizing elements in formation of a TOM-TIM-preprotein supercomplex. EMBO J. *22*, 5370–5381.

Chacinska, A., Pfannschmidt, S., Wiedemann, N., Kozjak, V., Sanjuán Szklarz, L.K., Schulze-Specking, A., Truscott, K.N., Guiard, B., Meisinger, C., and Pfanner, N. (2004). Essential role of Mia40 in import and assembly of mitochondrial intermembrane space proteins. EMBO J. *23*, 3735–3746.

Chacinska, A., Koehler, C.M., Milenkovic, D., Lithgow, T., and Pfanner, N. (2009). Importing mitochondrial proteins: machineries and mechanisms. Cell *138*, 628–644.

Chatzi, A., Sideris, D.P., Katrakili, N., Pozidis, C., and Tokatlidis, K. (2013). Biogenesis of yeast Mia40 - uncoupling folding from import and atypical recognition features. FEBS J. *280*, 4960–4969.

Curran, S.P., Leuenberger, D., Oppliger, W., and Koehler, C.M. (2002). The Tim9p-Tim10p complex binds to the transmembrane domains of the ADP/ATP carrier. EMBO J. *21*, 942–953.

D'Silva, P.D., Schilke, B., Walter, W., Andrew, A., and Craig, E.A. (2003). J protein cochaperone of the mitochondrial inner membrane required for protein import into the mitochondrial matrix. Proc. Natl. Acad. Sci. USA *100*, 13839–13844.

Dabir, D.V., Leverich, E.P., Kim, S.K., Tsai, F.D., Hirasawa, M., Knaff, D.B., and Koehler, C.M. (2007). A role for cytochrome *c* and cytochrome *c* peroxidase in electron shuttling from Erv1. EMBO J. *26*, 4801–4811.

Dekker, P.J., Martin, F., Maarse, A.C., Bömer, U., Müller, H., Guiard, B., Meijer, M., Rassow, J., and Pfanner, N. (1997). The Tim core complex defines the number of mitochondrial translocation contact sites and can hold arrested preproteins in the absence of matrix Hsp70-Tim44. EMBO J. *16*, 5408–5419.

Emanuelsson, O., Brunak, S., von Heijne, G., and Nielsen, H. (2007). Locating proteins in the cell using TargetP, SignalP and related tools. Nat. Protoc. *2*, 953–971.

Endo, T., and Yamano, K. (2009). Multiple pathways for mitochondrial protein traffic. Biol. Chem. *390*, 723–730.

Fölsch, H., Guiard, B., Neupert, W., and Stuart, R.A. (1996). Internal targeting signal of the BCS1 protein: a novel mechanism of import into mitochondria. EMBO J. *15*, 479–487.

Gabriel, K., Milenkovic, D., Chacinska, A., Müller, J., Guiard, B., Pfanner, N., and Meisinger, C. (2007). Novel mitochondrial intermembrane space proteins as substrates of the MIA import pathway. J. Mol. Biol. *365*, 612–620.

Ghaemmaghami, S., Huh, W.K., Bower, K., Howson, R.W., Belle, A., Dephoure, N., O'Shea, E.K., and Weissman, J.S. (2003). Global analysis of protein expression in yeast. Nature *425*, 737–741.

Hu, J., Dong, L., and Outten, C.E. (2008). The redox environment in the mitochondrial intermembrane space is maintained separately from the cytosol and matrix. J. Biol. Chem. *283*, 29126–29134.

Huang, S., Ratliff, K.S., and Matouschek, A. (2002). Protein unfolding by the mitochondrial membrane potential. Nat. Struct. Biol. *9*, 301–307.

Jin, C., Myers, A.M., and Tzagoloff, A. (1997). Cloning and characterization of MRP10, a yeast gene coding for a mitochondrial ribosomal protein. Curr. Genet. *31*, 228–234.

Kellems, R.E., Allison, V.F., and Butow, R.A. (1975). Cytoplasmic type 80S ribosomes associated with yeast mitochondria. IV. Attachment of ribosomes to the outer membrane of isolated mitochondria. J. Cell Biol. *65*, 1–14.

Koc, E.C., Cimen, H., Kumcuoglu, B., Abu, N., Akpinar, G., Haque, M.E., Spremulli, L.L., and Koc, H. (2013). Identification and characterization of CHCHD1, AURKAIP1, and CRIF1 as new members of the mammalian mitochondrial ribosome. Front. Physiol. *4*, 183.

Kojer, K., Bien, M., Gangel, H., Morgan, B., Dick, T.P., and Riemer, J. (2012). Glutathione redox potential in the mitochondrial intermembrane space is linked to the cytosol and impacts the Mia40 redox state. EMBO J. *31*, 3169–3182.

Larsson, N.G. (2010). Somatic mitochondrial DNA mutations in mammalian aging. Annu. Rev. Biochem. *79*, 683–706.

Longen, S., Bien, M., Bihlmaier, K., Kloeppel, C., Kauff, F., Hammermeister, M., Westermann, B., Herrmann, J.M., and Riemer, J. (2009). Systematic analysis of the twin cx(9)c protein family. J. Mol. Biol. *393*, 356–368.

Meier, S., Neupert, W., and Herrmann, J.M. (2005). Conserved N-terminal negative charges in the Tim17 subunit of the TIM23 translocase play a critical role in the import of preproteins into mitochondria. J. Biol. Chem. *280*, 7777–7785.

Merz, S., and Westermann, B. (2009). Genome-wide deletion mutant analysis reveals genes required for respiratory growth, mitochondrial genome maintenance and mitochondrial protein synthesis in *Saccharomyces cerevisiae*. Genome Biol. *10*, R95.

Mesecke, N., Terziyska, N., Kozany, C., Baumann, F., Neupert, W., Hell, K., and Herrmann, J.M. (2005). A disulfide relay system in the intermembrane space of mitochondria that mediates protein import. Cell *121*, 1059–1069.

Milenkovic, D., Ramming, T., Müller, J.M., Wenz, L.S., Gebert, N., Schulze-Specking, A., Stojanovski, D., Rospert, S., and Chacinska, A. (2009). Identification of the signal directing Tim9 and Tim10 into the intermembrane space of mitochondria. Mol. Biol. Cell *20*, 2530–2539.

Mokranjac, D., Paschen, S.A., Kozany, C., Prokisch, H., Hoppins, S.C., Nargang, F.E., Neupert, W., and Hell, K. (2003). Tim50, a novel component of the TIM23 preprotein translocase of mitochondria. EMBO J. *22*, 816–825.

Naoé, M., Ohwa, Y., Ishikawa, D., Ohshima, C., Nishikawa, S., Yamamoto, H., and Endo, T. (2004). Identification of Tim40 that mediates protein sorting to the mitochondrial intermembrane space. J. Biol. Chem. *279*, 47815–47821.

Neupert, W., and Herrmann, J.M. (2007). Translocation of proteins into mitochondria. Annu. Rev. Biochem. *76*, 723–749.

O'Brien, T.W. (2002). Evolution of a protein-rich mitochondrial ribosome: implications for human genetic disease. Gene *286*, 73–79.

Sideris, D.P., and Tokatlidis, K. (2007). Oxidative folding of small Tims is mediated by site-specific docking onto Mia40 in the mitochondrial intermembrane space. Mol. Microbiol. *65*, 1360–1373.

Sideris, D.P., Petrakis, N., Katrakili, N., Mikropoulou, D., Gallo, A., Ciofi-Baffoni, S., Banci, L., Bertini, I., and Tokatlidis, K. (2009). A novel intermembrane space-targeting signal docks cysteines onto Mia40 during mitochondrial oxidative folding. J. Cell Biol. *187*, 1007–1022.

Smits, P., Smeitink, J.A., van den Heuvel, L.P., Huynen, M.A., and Ettema, T.J. (2007). Reconstructing the evolution of the mitochondrial ribosomal proteome. Nucleic Acids Res. *35*, 4686–4703.

van der Laan, M., Wiedemann, N., Mick, D.U., Guiard, B., Rehling, P., and Pfanner, N. (2006). A role for Tim21 in membrane-potential-dependent preprotein sorting in mitochondria. Curr. Biol. *16*, 2271–2276.

Vestweber, D., and Schatz, G. (1988). Point mutations destabilizing a precursor protein enhance its post-translational import into mitochondria. EMBO J. *7*, 1147–1151.

Vögtle, F.N., Wortelkamp, S., Zahedi, R.P., Becker, D., Leidhold, C., Gevaert, K., Kellermann, J., Voos, W., Sickmann, A., Pfanner, N., and Meisinger, C. (2009). Global analysis of the mitochondrial N-proteome identifies a processing peptidase critical for protein stability. Cell *139*, 428–439.

Weckbecker, D., Longen, S., Riemer, J., and Herrmann, J.M. (2012). Atp23 biogenesis reveals a chaperone-like folding activity of Mia40 in the IMS of mitochondria. EMBO J. *31*, 4348–4358.